Article:
Cao, K, Lesnic, D and Ismailov, MI (2021) Determination of the time-dependent thermal grooving coefficient. Journal of Applied Mathematics and Computing, 65 (1-2). pp. 199-221. ISSN: 1598-5865

https://doi.org/10.1007/s12190-020-01388-7

Determination of the time-dependent thermal grooving coefficient

Kai Cao*[1], Daniel Lesnic†[2], and Mansur I. Ismailov‡[3,4]

[1]School of Mathematics, Southeast University, Nanjing, 210096, P. R. China

[2]Department of Applied Mathematics, University of Leeds, Leeds, LS2 9JT, United Kingdom

[3]Department of Mathematics, Gebze Institute of Technology, Gebze, Kocaeli, 41400, Turkey

[4]Department of Mathematics, Khazar University, Baku, AZ1096, Azerbaijan

Abstract

Changes in morphology of a polycrystalline material may occur through interface motion under the action of a driving force. An important special case that is considered in this paper is the thermal grooving that occurs when a grain boundary intersects the flat surface of a recently solidified metal slab giving rise to the formation of a thin symmetric groove. In case the transient surface diffusion is the main forming mechanism this yields a fourth-order time-dependent partial differential equation with unknown time-dependent surface diffusivity. In order to determine it, the profile of the free grooving surface at a fixed location is recorded in time. The grooving boundaries are supported by self-adjoint boundary conditions. We provide sufficient conditions on the input data for which the resulting coefficient identification problem is proved to be well-posed. Furthermore, we develop a predictor-corrector finite-difference spline method for obtaining an accurate and stable numerical solution to the nonlinear coefficient identification problem. Numerical results illustrate the performance of the inversion of both exact and noisy data.

Keywords: inverse problems; fourth-order parabolic equation; thermal grooving coefficient; predictor-corrector method

Declarations: Not applicable.

MSC classification codes: 35R30, 65M32

*kcao@seu.edu.cn

†Corresponding author: D.Lesnic@leeds.ac.uk

‡mismailov@gtu.edu.tr

1 Introduction

The fourth-order derivative with respect to space occurs in in many physics, chemistry, biology and engineering applications. For instance, the quantitative theory of thermal grooving through surface diffusion mechanism [29], the free vibration in beams and shafts [15], the epitaxial thin film growth [22], and the long range effect of insects dispersal [10] lead to fourth-order parabolic partial differential equations. Moreover, in [39], the fourth-order parabolic equation was utilized to balance the trade-off between noise removal and edge preservation, and avoid the blocky effects in image processing. In addition, it also appears in the Cahn-Hilliard equation which describes the evolution of a conserved concentration field during phase separation [9], and in the Kuramoto–Sivashinsky equation which describes the incipient instabilities in a variety of physical and chemical systems, [24, 34].

The existence, uniqueness, regularity and asymptotic behavior of the strong or weak solutions to the fourth-order parabolic equations have been widely investigated, e.g. [22, 26, 33, 37, 38]. Meanwhile, many numerical schemes have been developed to obtain the solutions of the fourth-order parabolic equations numerically, such as the finite-difference method [28], the spline method [4] and the finite-element method [23].

Inverse problems for the higher-order equation of order $2m$, $m \in \mathbb{N}^*$,

$$u_t + (-1)^m a(x,t)\partial_x^{2m} u(x,t) = g(x,t)p + r(x,t), \quad (x,t) \in (0,L) \times (0,T), \tag{1.1}$$

were considered in [19] and [20] to determine the unknown right-hand side term $p(t)$ or $p(x)$, respectively from an integral observation. The well-posedness of these inverse problems were established even in the degenerate case when the coefficient $a(x,t)$ is allowed to vanish on a zero-measure set.

As a practical application important in characterising the strength and stability of polycrystalline materials, we consider the study of a groove that forms when a vertical grain boundary meets a horizontal free surface. This particularly occurs in the thermal treatment and metallization of electronic components of power modules, [16]. As a mathematical model, we consider the fourth-order time-dependent Mullins partial differential equation governing the thermal grooving by surface diffusion [29, 27], which is the characteristic mechanism for mass transport at special metal surfaces such as gold. For other metals such as magnesium, the mechanism of evaporation-condensation is more appropriate, and new analytical expressions of the groove profile and its depth have recently been derived by [17] for this case. Surface diffusion is also the principal mechanism for small-size grooves less than $10\mu m$ or for grooving temperatures much lower than the meting temperature of the material, [30]. As such, understanding and determining surface diffusion unlock further perspectives for the ion transport mechanism at nanoscale, explaining the wide range of reported lifetimes of metallic conductive filaments used in resitive switching devices, [36].

The inverse mathematical model corresponding to (1.1) with $m = 2$, $a(x,t) = B(t)$ and $g(x,t)p + r(x,t) = f(x,t)$, i.e. (2.3), consists of determining the time-dependent unknown coefficient $B(t)$ from some additional observations, when all other quantities and initial and boundary conditions are all specified (Section 2). In Section 3, the existence of the solution to the inverse problem is achieved by using the Fourier method and Schauder's fixed point theorem. In addition, the uniqueness and continuous dependence upon the overdetermined data for the solution can be obtained by using the

properties of the Volterra integral equation. Meanwhile, the predictor-corrector method [11] regularized by the cubic spline function method [35] is developed in Section 4 to obtain the unknown coefficient numerically. Two one-dimensional numerical examples are performed and discussed in Section 5. Finally, Section 6 highlights the conclusions of the paper.

2 Problem formulation

We solve the inverse problem of determining the time-dependent thermal grooving coefficient (i.e., the surface diffusivity) from the measurement of the profile at an intermediate spatial point. The grooving boundaries are supported by the conditions that are identical to those of Mullins' [29], which are self-adjoint boundary conditions.

On the assumption that the surface profile $u(x,t)$ has a small slope, i.e. $|u_x|<<1$, the nonlinear equation governing the surface diffusion given by, [29, 7],

$$u_t = -B\partial_x[(1+u_x^2)^{-1/2}\partial_x(u_{xx}/(1+u_x^2)^{3/2})], \tag{2.1}$$

where B is the thermal grooving coefficient, reduces to the fourth-order linear equation

$$u_t = -Bu_{xxxx}. \tag{2.2}$$

More advanced models of thermal grooving by surface diffusion have recently been revisited in [2]; we can also mention here the fractional sub-diffusion modelling given by $\partial_t^\alpha u = -Bu_{xxxx}$, where $\alpha \in (0,1]$, see [1, 18].

We consider the inverse problem of finding the time-dependent $B(t) > 0$ for $t \in [0,T]$, together with $u(x,t)$ satisfying

$$\begin{cases} u_t + B(t)u_{xxxx} = f(x,t), & (x,t) \in (0,1)\times(0,T] =: \Omega_T, \\ u_x|_{x=0} = 0, \quad u_{xxx}|_{x=0} = 0, & t \in [0,T], \\ u_x|_{x=1} = 0, \quad u_{xxx}|_{x=1} = 0, & t \in [0,T], \\ u|_{t=0} = \varphi(x), & x \in [0,1], \end{cases} \tag{2.3}$$

along with the measurement of the profile

$$u(x_0,t) = E(t), \quad t \in [0,T] \tag{2.4}$$

at a fixed point $x_0 \in [0,1]$. In the above model, the boundary $x=0$ corresponds to the origin (centre) of the groove at which the slope and the mass flux must be zero due to symmetry. The thermal grooving coefficient is given by

$$B = \frac{D_s\gamma_s\omega}{k_BT}, \tag{2.5}$$

where D_s is the surface diffusivity, γ_s is the surface energy, ω is the atomic volume, k_B is the Boltzmann constant and T is the absolute temperature.

In practice, surface diffusivity is measured using sophisticated methods of characterisation based on radiotracers, field ion microscopy or topographic techniques, see e.g. [31]. However, if an additional chemical phenomenon/treatment is taking place then,

the surface diffusion D_s depends on time and becomes unknown. In such a situation, the measurement of surface diffusivity depending on time becomes infeasible using the current state-of-the-art experimental procedures, but instead, as proposed in the study for the first time, one can consider the computational mathematics inversion for its determination. We also mention that, although interesting from the mathematical point of view, the case when B may depend on x is not very physical in our context and therefore, it is not considered herein. On the other hand, in a future work, it would make sense to consider identifying a piecewise constant thermal grooving coefficient corresponding to multiple grooves.

Let $B(t)$ for $t \in [0,T]$, be unknown belonging to the class of admissible functions

$$\mathcal{M} = \left\{ B(t) \in C[0,T];\ 0 < \underline{b} \le B(t) \le \bar{b} \text{ for all } t \in [0,T] \right\}, \tag{2.6}$$

where $\underline{b}$ and $\bar{b}$ are given fixed positive constants. The assumption $B(t) \ge \underline{b} > 0$ for all $t \in [0,T]$ is physical because the themal grroving coefficient defined by (2.5) involves material properties, which are strictly positive quantities in normal conditions. However, in anomalous cases where the surface diffsivity may vanish (e.g. at the initial time $t = 0$), the PDE in (2.3) becomes degenerate and the techniques of [19, 20] may be applied. The solution $(B(t), u(x,t))$ of the inverse problem (2.3) and (2.4) is sought in the class $\mathcal{M} \times (C^{4,1}(\Omega_T) \cap C^{3,0}(\bar{\Omega}_T))$.

3 Well-posedness of the solution to the inverse problem

Corresponding to (2.3), we consider the fourth-order auxiliary spectral problem

$$\begin{cases} y''''(x) = \lambda y(x), \quad x \in [0,1], \\ y'(0) = 0, \quad y'''(0) = 0, \\ y'(1) = 0, \quad y'''(1) = 0, \end{cases} \tag{3.1}$$

which is self-adjoint in $L^2(0,1)$. Simple calculations yields the eigenvalues and normalized eigenfunctions

$$\lambda_0 = 0, \lambda_n = (\pi n)^4,\ y_0(x) = 1, y_n(x) = \sqrt{2}\cos(\pi n x),\ n \in \mathbb{N}^*,$$

of the fourth order differential operator.

Let us introduce the following classes of functions

$$D_1[0,1] \equiv \left\{ y \in C^5[0,1] : y'(0) = y'''(0) = y'(1) = y'''(1) = 0 \right\},$$
$$D_2[0,1] \equiv \left\{ y \in C^9[0,1] : y, y^{(4)} \in D_1[0,1] \right\}.$$

Lemma 3.1. *For $\varphi(x) \in D_k[0,1]$, the inequality*

$$\sum_{n=1}^{\infty} \lambda_n^k |\varphi_n| \le \frac{1}{\sqrt{6}} \left\| \varphi^{(4k+1)} \right\|_{L^2(0,1)}$$

holds for $k = 1$ and 2.

Proof. Using integration by parts, it is clear that

$$\lambda_n^k \varphi_n = (\varphi^{(4k)}, y_n) = -\frac{1}{\pi n}(\varphi^{(4k+1)}, z_n), \quad n \in \mathbb{N}^*$$

where $z_n = \sqrt{2}\sin(\pi n x)$ and $(\cdot,\cdot)$ denotes the inner product in $L^2(0,1)$. Then,

$$\begin{aligned}\sum_{n=1}^{\infty} \lambda_n^k |\varphi_n| =& \sum_{n=1}^{\infty} \frac{1}{\pi n} |(\varphi^{(4k+1)}, z_n)| \\ \leq& \frac{1}{\pi}\left(\sum_{n=1}^{\infty} \frac{1}{n^2}\right)^{\frac{1}{2}} \left(\sum_{n=1}^{\infty} \left|(\varphi^{(4k+1)}, z_n)\right|^2\right)^{\frac{1}{2}} \leq c \left\|\varphi^{(4k+1)}\right\|_{L^2(0,1)}\end{aligned}$$

holds with $c = \frac{1}{\pi}\sqrt{\sum_{n=1}^{\infty} \frac{1}{n^2}} = \frac{1}{\sqrt{6}}$, where we have used the Bessel and Cauchy-Schwartz inequalities. □

The well-posedness of solution of the inverse problem (2.3) and (2.4) is presented in the following theorems.

Theorem 3.1 (Existence of solution)**.** *Denote by* $\varphi_n := (\varphi, y_n) = \int_0^1 \varphi(x) y_n(x) dx$ *and* $f_n(t) := \int_0^1 f(x,t) y_n(x) dx$ *for* $n \in \mathbb{N}$*, and let the following conditions be satisfied:*

(i) $\varphi \in D_2[0,1]$ *with* $\cos(\pi n x_0)\varphi_n \geq 0$ *for all* $n \in \mathbb{N}$*, and there exists* $n_0 \in \mathbb{N}^*$ *such that* $\cos(\pi n_0 x_0)\varphi_{n_0} > 0$*;*

(ii) $E \in C^1[0,T]$ *with* $E(t) > \varphi_0 + \int_0^T f_0(\tau) d\tau$*,* $E'(t) < 0$ *for all* $t \in [0,T]$*, and* $E(0) = \varphi(x_0)$*;*

(iii) $f \in C(\overline{\Omega}_T)$*, and* $f(\cdot,t) \in D_2[0,1]$ *with* $\cos(\pi n x_0) f_n(t) \geq 0$ *for all* $t \in [0,T]$ *and* $n \in \mathbb{N}$*.*

Then, the inverse problem (2.3) *and* (2.4) *has a classical solution. Moreover,* $u(x,t) \in C^{4,1}(\bar{\Omega}_T)$*.*

Proof. To construct the formal solution of the problem (2.3) for arbitrary $B(t) \in C[0,T]$, we will use the Fourier series in terms of the eigenfunctions $y_n(x) = \sqrt{2}\cos(\pi n x)$, $n \in \mathbb{N}$, of the auxiliary spectral problem (3.1):

$$u(x,t) = \sum_{n=0}^{\infty} \left[\varphi_n e^{-\lambda_n \int_0^t B(s)ds} + \int_0^t f_n(\tau) e^{-\lambda_n \int_\tau^t B(s)ds} d\tau\right] y_n(x). \tag{3.2}$$

Because of the convergence the series $\sum_{n=0}^{\infty} \lambda_n |\varphi_n|$ and $\sum_{n=0}^{\infty} \lambda_n |f_n(\tau)|$, as given by Lemma 3.1, the function (3.2), its t-partial derivative and $xxxx$-fourth order partial derivative are continuous in Ω_T. Also, the function (3.2), its x-first and xxx-third order partial derivative are continuous in $\overline{\Omega}_T$. It means that the function $u(x,t)$ defined by the series (3.2) belongs to the class $C^{4,1}(\Omega_T) \cap C^{3,0}(\bar{\Omega}_T)$ and satisfies (2.3).

It can analogously be shown that the series (3.2) can be termwise continuously differentiated with t and that the series

$$u_t(x,t) \sim -\sum_{n=0}^{\infty} \left[\lambda_n \varphi_n B(t) e^{-\lambda_n \int_0^t B(s)ds} - f_n(t) + \lambda_n B(t) \int_0^t f_n(\tau) e^{-\lambda_n \int_\tau^t B(s)ds} d\tau\right] y_n(x) \tag{3.3}$$

is uniformly convergent. Then, differentiating (2.4) with respect to t and using (3.3) yield an for $B(t)$ given by:

$$\begin{aligned}&-\sqrt{2}B(t)\sum_{n=0}^{\infty}\lambda_n\left[\varphi_n e^{-\lambda_n\int_0^t B(s)ds}+\int_0^t f_n(\tau)e^{-\lambda_n\int_\tau^t B(s)ds}d\tau\right]\cos(\pi n x_0)\\ =&E'(t)-\sum_{n=0}^{\infty}f_n(t)y_n(x_0),\quad t\in[0,T],\end{aligned}$$

or

$$B=\Phi(B), \tag{3.4}$$

where

$$\Phi(B(t))=\frac{f(x_0,t)-E'(t)}{\sqrt{2}\sum\limits_{n=1}^{\infty}\lambda_n\left[\varphi_n e^{-\lambda_n\int_0^t B(s)ds}+\int_0^t f_n(\tau)e^{-\lambda_n\int_\tau^t B(s)ds}d\tau\right]\cos(\pi n x_0)}, \tag{3.5}$$

where we have used that $\sum_{n=0}^{\infty}f_n(t)y_n(x_0)=f(x_0,t)$. Let us denote

$$\underline{b}=\frac{\min\limits_{t\in[0,T]}f(x_0,t)-\max\limits_{t\in[0,T]}E'(t)}{C},\quad \overline{b}=\frac{\max\limits_{t\in[0,T]}f(x_0,t)-\min\limits_{t\in[0,T]}E'(t)}{E(T)-\varphi_0-\int_0^T f_0(\tau)d\tau}, \tag{3.6}$$

where $C=\left(\|\varphi^{(5)}\|_{L^2(0,1)}+\int_0^T\left\|\frac{\partial^5 f}{\partial x^5}(\cdot,t)\right\|_{L^2(0,1)}dt\right)/\sqrt{6}$. It is clear from (3.5), (3.6) and Lemma 3.1 that Φ maps the set $\mathcal{M}$ onto itself, i.e., $\Phi:\mathcal{M}\to\mathcal{M}$. Since $\mathcal{M}$ is bounded it follows that Φ is uniformly bounded. According to the Arzela theorem, we establish the equicontinuity of the function Φ. For this purpose, we take an arbitrary $\varepsilon>0$ and establish the existence of $\delta>0$ such that

$$|\Phi(B(t_1))-\Phi(B(t_2))|<\varepsilon \text{ for } |t_1-t_2|<\delta. \tag{3.7}$$

Using (3.5) we have that

$$|\Phi(B(t_1))-\Phi(B(t_2))|\le\frac{|K(t_1)-K(t_2)|}{N(t_2)}+\frac{|K(t_1)(N(t_1)-N(t_2))|}{N(t_1)N(t_2)}, \tag{3.8}$$

where $K(t)=f(x_0,t)-E'(t)$ and

$$N(t)=\sqrt{2}\sum_{n=0}^{\infty}\lambda_n\left[\varphi_n e^{-\lambda_n\int_0^t B(s)ds}+\int_0^t f_n(\tau)e^{-\lambda_n\int_\tau^t B(s)ds}d\tau\right]\cos(\pi n x_0).$$

By using the inequality

$$|e^{-\lambda_n\int_\tau^{t_1}B(s)ds}-e^{-\lambda_n\int_\tau^{t_2}B(s)ds}|\le\lambda_n|t_1-t_2|\max_{t\in[0,T]}B(t)$$

we obtain

$$|N(t_1)-N(t_2)|\le\alpha|t_1-t_2|, \tag{3.9}$$

where

$$\alpha = \sqrt{2}\left[\bar{b}\sum_{n=0}^{\infty}\lambda_n^2\left(|\varphi_n| + \int_0^T |f_n(\tau)|d\tau\right) + \sum_{n=0}^{\infty}\lambda_n \max_{t\in[0,T]}|f_n(t)|\right]. \tag{3.10}$$

On the other hand, since $K(t)$ is continuous in the closed interval $[0,T]$, for any $\varepsilon > 0$ there exists $\delta_1 = \delta_1(\varepsilon) > 0$ such that

$$|K(t_1) - K(t_2)| \leq \frac{\varepsilon}{2}\left(E(T) - \varphi_0 - \int_0^T f_0(\tau)d\tau\right) \tag{3.11}$$

for all t_1 and t_2 in $[0,T]$ for which $|t_1 - t_2| < \delta_1$. By choosing

$$\delta = \min\left\{\delta_1(\varepsilon), \frac{\left(E(T) - \varphi_0 - \int_0^T f_0(\tau)d\tau\right)^2}{\alpha\left(\max\limits_{t\in[0,T]} f(x_0,t) - \min\limits_{t\in[0,T]} E'(t)\right)}\frac{\varepsilon}{2}\right\}$$

from (3.8) we obtain (3.7). This shows that the operator Φ is uniformly bounded and equicontinuous. Using Schauder's fixed point theorem, we obtain that a solution $B(t) \in \mathcal{M}$ of the equation (3.4) exists. Substituting it in (3.2), we find that function $u = u(x,t)$ possesses the extra smoothness $u \in C^{4,1}(\overline{\Omega}_T)$. □

Remark 3.1. *The conditions (i)-(iii) of Theorem 3.1 are conditions on the input data φ, f and E for arbitrary fixed $x_0 \in [0,1]$. Some of these conditions are consistency conditions, e.g. $E(0) = \varphi(x_0)$ in (ii), that need to be satisfied to avoid non-physical discontinuous solutions. Others, like (i) and (iii) are sufficient conditions that ensure the positivity of the physical grooving coefficient $B(t)$. Moreover, since we use the Fourier series method we expect these conditions to appear in terms of the Fourier coefficients. Probably the more difficult to ensure are the remaining conditions $E' < 0$ and $E > \varphi_0 + \int_0^T f_0(\tau)d\tau$; however, for a given fixed arbitrary point $x_0 \in [0,1]$ we can easily check that the following input that satisfy all the conditions of Theorem 3.1 (and also of Theorem 3.2) (see also section 5.1 for another example):*
(i) if $x_0 = 0$, then consider $\varphi(x) = 1 + \cos(\pi n_0 x)$, $f(x,t) = e^t\cos(\pi n_0 x)$ and $E(t) = 1 - e^{-t}$ for any fixed $n_0 \in \mathbb{N}^*$;
(ii) if $x_0 \in (0,1]$, then consider $\varphi(x) = 1 - \cos(\pi n_0 x)$, $f(x,t) = -e^t\cos(\pi n_0 x)$ and $E(t) = 1 + e^{-t}\cos(\pi n_0 x_0)$ for $n_0 = [2.5/x_0] + 1$, where $[\cdot]$ denotes the integer part of a number.

Theorem 3.2 (Uniqueness of solution)**.** *Let the following conditions be satisfied:*
(iv) $\varphi \in D_1[0,1]$;
(v) $E \in C^1[0,T]$ with $E(0) = \varphi(x_0)$;
(vi) $f \in C(\overline{\Omega}_T)$ and $f(\cdot,t) \in D_1[0,1]$ with $f(x_0,t) \neq E'(t)$ for all $t \in [0,T]$.
Then, the solution of the inverse problem (2.3) and (2.4) is unique.

Proof. Assume that there exist two solutions $(B_i(t), u^{(i)}(x,t))$, $i = 1,2$, of the inverse problem (2.3) and (2.4). For the difference of these solutions $B(t) = B_2(t) - B_1(t)$,

$u(x,t) = u^{(1)}(x,t) - u^{(2)}(x,t)$, we obtain the following problem:

$$\begin{cases} u_t + B_1(t)u_{xxxx} = B(t)u^{(2)}_{xxxx}, & (x,t) \in \Omega_T, \\ u_x|_{x=0} = 0, \quad u_{xxx}|_{x=0} = 0, & t \in [0,T], \\ u_x|_{x=1} = 0, \quad u_{xxx}|_{x=1} = 0, & t \in [0,T], \\ u|_{t=0} = 0, & x \in [0,1]. \end{cases} \tag{3.12}$$

Using that $u(x_0,t) = 0$ for $t \in [0,T]$, from the first equation in (3.12) we obtain

$$B_1(t)u_{xxxx}(x_0,t) = B(t)u^{(2)}_{xxxx}(x_0,t). \tag{3.13}$$

Using the Fourier series representation of the solution of (3.12), identity (3.13) recasts as

$$\sqrt{2}B_1(t)\sum_{n=0}^{\infty}\lambda_n\cos(\pi n x_0)\int_0^t B(\tau)\left(u^{(2)}_{xxxx}\right)_n(\tau)e^{-\lambda_n\int_\tau^t B_1(s)ds}d\tau = B(t)u^{(2)}_{xxxx}(x_0,t), \quad t \in [0,T],$$

where $(u^{(2)}_{xxxx})_n(t) := (u^{(2)}_{xxxx}, y_n)$.

Using that $u^{(2)}_{xxxx}(x_0,t) = \frac{f(x_0,t)-E'(t)}{B_2(t)} \neq 0$ for all $t \in [0,T]$, from assumption (vi), we can represent (3.14) in the form of a homogeneous Volterra integral equation for B, namely,

$$B(t) + \int_0^t K(t,\tau)B(\tau)d\tau = 0, \tag{3.14}$$

where

$$K(t,\tau) = -\frac{\sqrt{2}B_1(t)B_2(t)\sum_{n=0}^{\infty}\lambda_n\cos(\pi n x_0)(u^{(2)}_{xxxx})_n(\tau)e^{-\lambda_n\int_\tau^t B_1(s)ds}}{f(x_0,t)-E'(t)}. \tag{3.15}$$

The kernel $K(t,\tau)$ is continuous. In view of the properties of Volterra integral equations of the second kind, see e.g. [8], equation (3.14) has only the trivial solution $B(t) \equiv 0$. Therefore, $B(t) \equiv 0$ for all $t \in [0,T]$, and $u(x,t) \equiv 0$ for all $(x,t) \in \Omega_T$, as a solution of problem (3.12). □

Remark 3.2. *The identification of the thermal grooving coefficient $B(t)$ from the measurement of the total mass/energy*

$$\int_0^1 u(x,t)dx = \mathrm{E}(t), \quad t \in [0,T], \tag{3.16}$$

can also be considered, but this determination is not unique. This can easily be seen as follows. By integrating (3.2) with respect to x from 0 to 1 we obtain that $E(t) = \varphi_0 + \int_0^t f_0(\tau)d\tau$ is a necessary condition for the component $u(x,t)$ of solution to the inverse problem (2.3) and (3.16) to exist. However, because this condition does not depend on $B(t)$, it does not contain any information to enforce in order to obtain the uniqueness of the component $B(t)$ of solution.

Remark 3.3. *In the thermal grooving process proposed in [3], the grooving boundary conditions are zero flux and zero curvature at the root, namely $u_x|_{x=0} = 0$, $u_{xx}|_{x=0} = 0$. In this case, the relevant spectral problem is not self-adjoint for any given boundary condition at $x = 1$, and the classical theory [12] of expansion in terms of eigenfunctions for self-adjoint differential operators is not applicable.*

Justified by the assumptions (ii) and (iii), let us introduce the following class for the additional data (2.4):

$$\Sigma := \left\{ \begin{array}{ll} E \in C^1[0,T]; & 0 < M_0 \leq E(t) - \varphi_0 - \int_0^t f_0(\tau)d\tau, \\ & 0 < M_1 \leq f(x_0,t) - E'(t) \leq M_2 \text{ for all } t \in [0,T] \end{array} \right\}, \quad (3.17)$$

where M_0, M_1 and M_2 are given fixed positive constants. Then, it is easy to show from (3.4) and (3.5) that

$$\underline{b} := \frac{M_1}{\sqrt{2}\sum_{n=0}^{\infty}\lambda_n\left[|\varphi_n| + \int_0^T |f_n(\tau)|d\tau\right]} \leq B(t) \leq \frac{M_2}{M_0} = \bar{b}. \quad (3.18)$$

The continuous dependence upon the overdetermined data $E \in \Sigma$ of the solution of the inverse problem (2.3) and (2.4) is given in the following theorem.

Theorem 3.3 (Continuous dependence upon the overdetermined data)**.** *Let the assumptions (i)-(iii) of Theorem 3.1 be satisfied. Then the solution of the inverse problem* (2.3) *and* (2.4) *depends continuously upon the measurement data E in Σ.*

Proof. Let $(B_i(t), u^{(i)}(x,t))$, $i = 1, 2$, be the solutions of problem (2.3) and (2.4) with same initial data $\varphi(x)$ and free term $f(x,t)$, but different measurement data $E_1(t)$ and $E_2(t)$ from the class Σ. For the difference of these solutions $B(t) := B_2(t) - B_1(t)$, $u(x,t) := u^{(1)}(x,t) - u^{(2)}(x,t)$, we obtain the problem same as (3.12) with the overdetermination condition

$$u(x_0,t) = E_1(t) - E_2(t), \quad t \in [0,T]. \quad (3.19)$$

Differentiating in (3.19) and using the first equation in (3.12) we obtain

$$E_1'(t) - E_2'(t) + B_1(t)u_{xxxx}(x_0,t) = B(t)u^{(2)}_{xxxx}(x_0,t). \quad (3.20)$$

Using the Fourier series representation of the solution of (3.12), identity (3.20) recasts as

$$\begin{aligned} &E_1'(t) - E_2'(t) + \sqrt{2}B_1(t)\sum_{n=0}^{\infty}\lambda_n\cos(\pi n x_0)\int_0^t B(t)\left(u^{(2)}_{xxxx}\right)_n(\tau)e^{-\lambda_n\int_\tau^t B_1(s)ds}d\tau \\ =&B(t)u^{(2)}_{xxxx}(x_0,t). \end{aligned} \quad (3.21)$$

As in obtaining (3.14), using that $u^{(2)}_{xxxx}(x_0,t) = \frac{f(x_0,t)-E_2'(t)}{B_2(t)}$, we can represent (3.21) in the form of an inhomogeneous Volterra integral equation for B, namely,

$$B(t) + \int_0^t K(t,\tau)B(\tau)d\tau = g(t), \quad (3.22)$$

where $K(t,\tau)$ is given by (3.15) and

$$g(t) = \frac{(E_1'(t) - E_2'(t))\,B_2(t)}{f(x_0,t) - E_2'(t)}.$$

The kernel $K(t,\tau)$ and the free term $g(t)$ are continuous. In view of the properties of Volterra integral equations of the second kind, equation (3.22) has a unique continuous solution $B(t)$. On using (2.3), (3.3), (3.15) and (3.17), the estimates

$$|K(t,\tau)| \leq \frac{2\bar{b}^2}{M_1} \sum_{n=0}^{\infty} \lambda_n^2 \left[|\varphi_n| + \int_0^T |f_n(s)| ds \right], \tag{3.23}$$

$$|g(t)| \leq \frac{\bar{b}}{M_1} \|E_1 - E_2\|_{C^1[0,T]}, \tag{3.24}$$

hold for the kernel $K(t,\tau)$ and the free term $g(t)$. Then, using (3.22) we obtain

$$|B(t)| \leq \frac{\bar{b}}{M_1} \|E_1 - E_2\|_{C^1[0,T]} + \frac{2\bar{b}^2}{M_1} \int_0^t \sum_{n=0}^{\infty} \lambda_n^2 \left[|\varphi_n| + \int_0^T |f_n(s)| ds \right] |B(\tau)| d\tau.$$

Then, by using the integral form of Gronwall's inequality, we obtain that $B(t) = B_2(t) - B_1(t)$ satisfies the stability estimate

$$\|B_1 - B_2\|_{C[0,1]} \leq \frac{\bar{b}}{M_1} e^{mT} \|E_1 - E_2\|_{C^1[0,T]} \tag{3.25}$$

where

$$m = \frac{2\bar{b}^2}{M_1} \sum_{n=0}^{\infty} \lambda_n^2 \left[|\varphi_n| + \int_0^T |f_n(s)| ds \right].$$

This inequality implies the continuous dependence of B upon the overdetermined data E. Using a similar proof to the above it can we can prove that u, which is given in (3.2), depends continuously upon the data. □

The stability estimate (3.25) is valid for smooth measured data (2.4) in $C^1[0,T]$. However, in practice such data is seldom smooth and therefore, the inverse problem is likely to be ill-posed if the data (2.4) is in $C[0,T]$ only and not in $C^1[0,T]$. In such a situation, regularization is necessary, as described in the next section.

4 Predictor-corrector method

In this section, we consider the numerical reconstruction of the unknown thermal grooving coefficient $B(t)$ using the predictor–corrector method [11] combined with the finite-difference scheme. We first establish the finite-difference method (FDM) to obtain the numerical solution of the direct initial-boundary value problem:

$$\begin{cases} u_t + B(t) u_{xxxx} = f(x,t), & (x,t) \in (0,L) \times (0,T], \\ u_x|_{x=0} = \eta_0(t), \quad u_{xxx}|_{x=0} = \gamma_0(t), & t \in [0,T], \\ u_x|_{x=1} = \eta_1(t), \quad u_{xxx}|_{x=1} = \gamma_1(t), & t \in [0,T], \\ u(x,0) = \varphi(x), & x \in [0,L], \end{cases} \tag{4.1}$$

where $B(t) > 0$ is known, and the main dependent variable to be determined is the function $u(x,t)$. The problem (4.1) becomes (2.3), which is investigated in this work,

if $L = 1$ and the boundary conditions satisfy $\eta_0(t) = \eta_1(t) = \gamma_0(t) = \gamma_1(t) = 0$ for $t \in [0, T]$.

Divide the domain $[0, L] \times [0, T]$ into the following uniform grid:

$$x_i = (i-1)h, \quad i = \overline{1, I}, \quad t_k = (k-1)\tau, \quad k = \overline{1, K},$$

where $h = \frac{L}{I-1}$ and $\tau = \frac{T}{K-1}$ are space and time mesh step sizes, and denote the values of $u(x,t)$, $B(t)$, $f(x,t)$, $\eta_1(t)$, $\eta_1(t)$, $\gamma_0(t)$, $\gamma_1(t)$ and $\varphi(x)$ at the node (i,k) by:

$$u_i^k = u(x_i, t_k), \quad f_i^k = f(x_i, t_k), \quad B^k = B(t_k), \quad \varphi_i = \varphi(x_i),$$
$$\eta_0^k = \eta_0(t_k), \quad \eta_1^k = \eta_1(t_k), \quad \gamma_0^k = \gamma_0(t_k), \quad \gamma_1^k = \gamma_1(t_k).$$

Defining

$$f_i^{k-\frac{1}{2}} = \frac{f_i^k + f_i^{k-1}}{2}, \quad \delta_t u_i^{k-\frac{1}{2}} = \frac{u_i^k - u_i^{k-1}}{\tau},$$
$$\delta_x^2 u_i^k = \frac{u_{i-1}^k - 2u_i^k + u_{i+1}^k}{h^2}, \quad \delta_x^4 u_i^k = \delta_x^2(\delta_x^2 u_i^k),$$

we obtain the Crank-Nicolson scheme for the initial-boundary value problem (4.1), as follows:

$$\begin{cases} \delta_t u_i^{k-\frac{1}{2}} + \frac{1}{2} B^{k-\frac{1}{2}} (\delta_x^4 u_i^k + \delta_x^4 u_i^{k-1}) = f_i^{k-\frac{1}{2}}, & i = \overline{2, I-1}, k = \overline{2, K}, \\ u_1^k = \frac{1}{3}(4u_2^k - u_3^k - 2h\eta_0^k), & k = \overline{2, K}, \\ u_I^k = \frac{1}{3}(4u_{I-1}^k - u_{I-2}^k + 2h\eta_1^k), & k = \overline{2, K}, \\ u_i^1 = \varphi_i, & i = \overline{1, I}. \end{cases} \tag{4.2}$$

The centred finite-difference formula for five-point stencils (of order $O(h^2)$) approximating the fourth-order derivative term $\delta_x^4 u_i^k$ for $i = \overline{4, I-3}$ and $k = \overline{2, K}$, in (4.2) can be written as

$$\begin{aligned} \delta_x^4 u_i^k =& \delta_x^2(\delta_x^2 u_i^k) = \delta_x^2 \left(\frac{1}{h^2}(u_{i-1}^k - 2u_i^k + u_{i+1}^k) \right) \\ =& \frac{1}{h^4}(u_{i-2}^k - 4u_{i-1}^k + 6u_i^k - 4u_{i+1}^k + u_{i+2}^k). \end{aligned} \tag{4.3}$$

Other time-stepping algorithms based on the method of lines, [25], as well as the three-point biharmonic compact operator, [14], or the orthogonal spline collocation, [5, 6], methods could be interesting alternatives.

For $i = 3$, $i = I-2$ and $k = \overline{2, K}$, using the second and third identities of (4.2), we have

$$\delta_x^4 u_3^k = \frac{1}{h^4}(u_1^k - 4u_2^k + 6u_3^k - 4u_4^k + u_5^k) = \frac{1}{h^4} \left(-\frac{8}{3}u_2^k + \frac{17}{3}u_3^k - 4u_4^k + u_5^k - \frac{2h}{3}\eta_0^k \right), \tag{4.4}$$

$$\begin{aligned} \delta_x^4 u_{I-2}^k =& \frac{1}{h^4}(u_{I-4}^k - 4u_{I-3}^k + 6u_{I-2}^k - 4u_{I-1}^k + u_I^k) \\ =& \frac{1}{h^4} \left(u_{I-4}^k - 4u_{I-3}^k + \frac{17}{3}u_{I-2}^k - \frac{8}{3}u_{I-1}^k + \frac{2h}{3}\eta_1^k \right). \end{aligned} \tag{4.5}$$

We now consider $\delta_x^2 u_1^k$ before giving the formulation of $\delta_x^4 u_2^k$. Using Taylor's expansion, we have

$$u_{xx}(h,t) = u_{xx}(0,t) + hu_{xxx}(0,t) + \frac{h^2}{2}u_{xxxx}(0,t) + o(h^2),$$
$$u_{xx}(2h,t) = u_{xx}(0,t) + 2hu_{xxx}(0,t) + \frac{4h^2}{2}u_{xxxx}(0,t) + o(h^2),$$

which implies that

$$u_{xx}(0,t) = \frac{1}{3}\left(4u_{xx}(h,t) - u_{xx}(2h,t) - 2h\gamma_0(t)\right) + o(h^2).$$

Then, we can obtain that

$$\delta_x^2 u_1^k = \frac{1}{3}(4\delta_x^2 u_2^k - \delta_x^2 u_3^k - 2h\gamma_0^k). \tag{4.6}$$

For $i = 2$ and $k = \overline{2, K}$, using (4.6) we get

$$\begin{aligned}\delta_x^4 u_2^k =& \delta_x^2(\delta_x^2 u_2^k) = \frac{1}{h^2}(\delta_x^2 u_1^k - 2\delta_x^2 u_2^k + \delta_x^2 u_3^k) = \frac{2}{3h^2}(-\delta_x^2 u_2^k + \delta_x^2 u_3^k - h\gamma_0^k)\\ =& \frac{2}{3h^4}(-u_1^k + 3u_2^k - 3u_3^k + u_4^k - h^3\gamma_0^k)\\ =& \frac{2}{3h^4}\left(\frac{5}{3}u_2^k - \frac{8}{3}u_3^k + u_4^k + \frac{2h}{3}\eta_0^k - h^3\gamma_0^k\right),\end{aligned} \tag{4.7}$$

and similarly, for $i = I-1$ and $k = \overline{2, K}$, we have

$$\delta_x^2 u_I^k = \frac{1}{3}(4\delta_x^2 u_{I-1}^k - \delta_x^2 u_{I-2}^k + 2h\gamma_1^k),$$

and

$$\begin{aligned}\delta_x^4 u_{I-1}^k =& \frac{1}{h^2}(\delta_x^2 u_{I-2}^k - 2\delta_x^2 u_{I-1}^k + \delta_x^2 u_I^k) = \frac{2}{3h^2}(\delta_x^2 u_{I-2}^k - \delta_x^2 u_{I-1}^k + h\gamma_1^k)\\ =& \frac{2}{3h^4}(u_{I-3}^k - 3u_{I-2}^k + 3u_{I-1}^k - u_I^k + h^3\gamma_1^k)\\ =& \frac{2}{3h^4}\left(u_{I-3}^k - \frac{8}{3}u_{I-2}^k + \frac{5}{3}u_{I-1}^k - \frac{2h}{3}\eta_1^k + h^3\gamma_1^k\right).\end{aligned} \tag{4.8}$$

Using (4.3)–(4.5), (4.7) and (4.8), the difference equation (4.2) can be reformulated as a $(I-2)\times(I-2)$ system of linear algebraic equations of the form

$$\begin{cases}\mathcal{A}^{k-1}\mathbf{u}^k = \mathcal{B}^{k-1}\mathbf{u}^{k-1} + \mathbf{F}^{k-1}, & k = \overline{2, K},\\ u_1^k = \frac{1}{3}(4u_2^k - u_3^k - 2h\eta_0^k), & k = \overline{2, K},\\ u_I^k = \frac{1}{3}(4u_{I-1}^k - u_{I-2}^k + 2h\eta_1^k), & k = \overline{2, K},\\ \mathbf{u}^1 = \left[\varphi_1, \varphi_2, \cdots, \varphi_I\right]^{\mathrm{T}},\end{cases} \tag{4.9}$$

where $\mathbf{u}^k = \left[u_2^k, u_3^k, \cdots, u_{I-1}^k\right]^{\mathrm{T}}$, and the $(I-2)\times(I-2)$ tridiagonal matrices $\mathcal{A}^{k-1}$ and $\mathcal{B}^{k-1}$ and the vector $\mathbf{F}^{k-1}$ are given by

$$\mathcal{A}^{k-1} = \begin{bmatrix} 1+\frac{10}{9}r^{k-\frac{1}{2}} & -\frac{16}{9}r^{k-\frac{1}{2}} & \frac{2}{3}r^{k-\frac{1}{2}} & & & & \\ -\frac{8}{3}r^{k-\frac{1}{2}} & 1+\frac{17}{3}r^{k-\frac{1}{2}} & -4r^{k-\frac{1}{2}} & r^{k-\frac{1}{2}} & & & \\ r^{k-\frac{1}{2}} & -4r^{k-\frac{1}{2}} & 1+6r^{k-\frac{1}{2}} & -4r^{k-\frac{1}{2}} & & & \\ & \ddots & \ddots & \ddots & \ddots & & \\ & & r^{k-\frac{1}{2}} & -4r^{k-\frac{1}{2}} & -4r^{k-\frac{1}{2}} & r^{k-\frac{1}{2}} & \\ & & & r^{k-\frac{1}{2}}1+\frac{17}{3}r^{k-\frac{1}{2}} & -\frac{8}{3}r^{k-\frac{1}{2}} & & \\ & & & & -\frac{16}{9}r^{k-\frac{1}{2}} & 1+\frac{10}{9}r^{k-\frac{1}{2}} \end{bmatrix},$$

$$\mathcal{B}^{k-1} = \begin{bmatrix} 1-2r^{k-\frac{1}{2}} & 2r^{k-\frac{1}{2}} & -\frac{2}{3}r^{k-\frac{1}{2}} & & & & \\ 4r^{k-\frac{1}{2}} & 1-6r^{k-\frac{1}{2}} & 4r^{k-\frac{1}{2}} & -r^{k-\frac{1}{2}} & & & \\ -r^{k-\frac{1}{2}} & 4r^{k-\frac{1}{2}} & 1-6r^{k-\frac{1}{2}} & 4r^{k-\frac{1}{2}} & -r^{k-\frac{1}{2}} & & \\ & \ddots & \ddots & \ddots & \ddots & \ddots & \\ & & -r^{k-\frac{1}{2}} & 4r^{k-\frac{1}{2}} & 1-6r^{k-\frac{1}{2}} & 4r^{k-\frac{1}{2}} & -r^{k-\frac{1}{2}} \\ & & & -r^{k-\frac{1}{2}} & 4r^{k-\frac{1}{2}} & 1-6r^{k-\frac{1}{2}} & 4r^{k-\frac{1}{2}} \\ & & & & -\frac{2}{3}r^{k-\frac{1}{2}} & 2r^{k-\frac{1}{2}} & 1-2r^{k-\frac{1}{2}} \end{bmatrix},$$

and

$$\mathbf{F}^{k-1} = \begin{bmatrix} \tau f_2^{k-\frac{1}{2}} + \frac{2}{3}r^{k-\frac{1}{2}}u_1^{k-1} - \frac{4}{9}hr^{k-\frac{1}{2}}\eta_0^k + \frac{2h^3}{3}r^{k-\frac{1}{2}}(\gamma_0^k + \gamma_0^{k-1}) \\ \tau f_3^{k-\frac{1}{2}} - r^{k-\frac{1}{2}}u_1^{k-1} + \frac{2}{3}hr^{k-\frac{1}{2}}\eta_0^k \\ \tau f_4^{k-\frac{1}{2}} \\ \cdots \\ \tau f_{I-3}^{k-\frac{1}{2}} \\ \tau f_{I-2}^{k-\frac{1}{2}} - r^{k-\frac{1}{2}}u_I^{k-1} - \frac{2}{3}hr^{k-\frac{1}{2}}\eta_1^k \\ \tau f_{I-1}^{k-\frac{1}{2}} + \frac{2}{3}r^{k-\frac{1}{2}}u_I^{k-1} + \frac{4}{9}hr^{k-\frac{1}{2}}\eta_1^k - \frac{2h^3}{3}r^{k-\frac{1}{2}}(\gamma_1^k + \gamma_1^{k-1}) \end{bmatrix},$$

where $r^{k-\frac{1}{2}} = \frac{\tau}{2h^4}B^{k-\frac{1}{2}} = \frac{\tau}{4h^4}(B^k + B^{k-1})$.

Theorem 4.1 ([32]). *If $u \in C^{6,3}((0,L)\times(0,T))$, the finite-difference scheme* (4.9) *to the initial-boundary value problem* (4.1) *is convergent with order $O(\tau^2 + h^2)$.*

Now, we construct the predicting-correcting mechanism to recover the unknown thermal grooving coefficient $B(t)$. Taking $x = x_0$, then (2.3) can be written as

$$E'(t) + B(t)u_{xxxx}(x_0, t) = f(x_0, t),$$

which formally yields that

$$B(t) = \frac{f(x_0,t) - E'(t)}{u_{xxxx}(x_0,t)}. \tag{4.10}$$

Then, the finite-difference approximation of $B^k = B(t_k)$ is

$$B^k = \frac{f_{I_0}^k - E_t^k}{(u_{xxxx})_{I_0}^k} = \frac{(f_{I_0}^k - E_t^k)h^4}{u_{I_0-2}^k - 4u_{I_0-1}^k + 6u_{I_0}^k - 4u_{I_0+1}^k + u_{I_0+2}^k}, \quad k = \overline{1,K}, \tag{4.11}$$

where $I_0 = \frac{x_0}{h} + 1$ and $E_t^k = E'(t^k)$.

Clearly, B^1 can be computed by the values of the initial data φ_i for $i = \overline{I_0 - 2, I_0 + 2}$. Suppose that $B^1, \cdots, B^k$ and u_i^k for $k = \overline{1, K-1}$ and $i = \overline{1, I}$, have been determined, we now present the algorithm [13, 21] to reconstruct B^{k+1}, $k = \overline{1, K-1}$, as follows:

Step 1. Since the time step τ is small, choose initial guesses $B^{k+1(0)}$ and $u_i^{k+1(0)}$ of B^{k+1} and u_i^{n+1} as $B^{k+1(0)} = B^k$ and $u_i^{k+1(0)} = u_i^k$, $k = \overline{1, K-1}$, $i = \overline{1, I}$.

Step 2. Calculate the update of B^{k+1} as

$$B^{k+1(1)} = \frac{(f_{I_0}^{k+1} - E_t^{k+1})h^4}{u_{I_0-2}^{k+1(0)} - 4u_{I_0-1}^{k+1(0)} + 6u_{I_0}^{k+1(0)} - 4u_{I_0+1}^{k+1(0)} + u_{I_0+2}^{k+1(0)}}.$$

Step 3. Compute the update of u^{k+1} by solving the following system of linear algebraic equations:

$$\begin{cases} \frac{u_i^{k+1(1)} - u_i^{k+1(0)}}{\tau} + \frac{B^{k+1(1)} + B^{k+1(0)}}{4}(\delta_x^4 u_i^{k+1(1)} + \delta_x^4 u_i^{k+1(0)}) = f_i^{k+\frac{1}{2}}, \quad i = \overline{2, I-1}, \\ u_1^{k+1(1)} = \frac{1}{3}(4u_2^{k+1(1)} - u_3^{k+1(1)} - 2h\eta_0^{k+1}), \\ u_I^{k+1(1)} = \frac{1}{3}(4u_{I-1}^{k+1(1)} - u_{I-2}^{k+1(1)} + 2h\eta_1^{k+1}). \end{cases}$$

Step 4. Compute the difference between two iterations, i.e. $|B^{k+1(1)} - B^{k+1(0)}|$, and choose an arbitrarily small positive constant γ, for instance $\gamma = h^3$, as the prescribed tolerance. If

$$|B^{k+1(1)} - B^{k+1(0)}| < \gamma \tag{4.12}$$

then take $B^{k+1} = B^{k+1(1)}$ and $u_i^{k+1} = u_i^{k+1(1)}$, $i = \overline{1, I}$, and go to **Step 5**. Else go to **Step 2** with the new initial guesses $B^{k+1(0)} = B^{k+1(1)}$ and $u_i^{k+1(0)} = u_i^{k+1(1)}$, $i = \overline{1, I}$.

Step 5. End.

For exact input data $E(t)$, its first-order derivative can be approximated by the difference quotients as follows:

$$E_t^1 = \frac{E^2 - E^1}{\tau}, \quad E_t^K = \frac{E^K - E^{K-1}}{\tau}, \quad E_t^k = \frac{E^{k+1} - E^{k-1}}{2\tau}, \quad k = \overline{2, K-1}. \tag{4.13}$$

However, in practice the measured data is noisy and given by a noisy perturbation E^ϵ of E satisfying

$$\|E^\epsilon - E\|_{C(0,T)} \leq \epsilon. \tag{4.14}$$

In such case, the finite difference (4.13) can only be employed for exact input data or when ϵ is very small. In general, the process of numerical differentiating of a noisy function is known to be ill-posed. In order to obtain a stable derivative of $E^\epsilon(t)$, formulae (4.13) need to be employed with $\tau = O(\sqrt{\epsilon})$. Alternatively, as described below, we can employ the cubic spline function method [35] to stably approximate the derivative of noisy input data E^ϵ.

The natural cubic spline $s(t)$ approximating the function $E(t)$ satisfies the following conditions:

(a) $s(t)$ is a twice differentiable natural cubic spline of time mesh grid t_k, i.e.

$$s(t_k+) = s(t_k-), \quad s'(t_k+) = s'(t_k-), \quad s''(t_k+) = s''(t_k-), \quad k = \overline{2, K-1},$$

where $s(t_k+) = \lim_{t \to t_k+} s(t)$ and $s(t_k-) = \lim_{t \to t_k-} s(t)$.

(b) $s''(0) = s''(T) = 0$.

(c) The third-order derivative of $s(t)$ at t_k satisfies the following conditions:

$$s'''(t_k+) - s'''(t_k-) = \frac{\tau}{\alpha}(E^\epsilon(t_k) - s(t_k)), \quad k = \overline{2, K-1},$$

where $\alpha > 0$ is the regularization parameter. The details of calculating $s(t)$ are presented in [13].

Theorem 4.2 ([35]). *Suppose that $E(t) \in H^2(0,T)$. Then, the function $s(t)$ obtained above satisfies the following estimate:*

$$\|s' - E'\|_{L^2(0,T)} \leq \left(2\tau + 4\alpha^{1/4} + \frac{\tau}{\pi}\right)\|s''\|_{L^2(0,T)} + \tau\frac{\alpha^{1/2}}{\epsilon} + \frac{2\epsilon}{\alpha^{1/2}}.$$

If $\alpha = \epsilon^2$, then

$$\|s' - E'\|_{L^2(0,T)} \leq \left(2\tau + 4\sqrt{\epsilon} + \frac{\tau}{\pi}\right)\|s''\|_{L^2(0,T)} + \tau + 2\sqrt{\epsilon}.$$

Remark 4.1. *The above theorem indicates that the regularization parameter α can be chosen as ϵ^2, and for the derivative of the noisy input data $E^\epsilon(t)$ we can use instead $s'(t)$. For exact data, formula (4.13) is employed instead of the cubic spline function method.*

5 Numerical results and discussions

In this section, we perform a couple of one-dimensional experiments to numerically reconstruct the time-dependent thermal grooving coefficient $B(t)$, based on the predictor-corrector method described in Section 4.

The measured data E^ϵ in (4.14) is simulated by adding Gaussian noise to the true data $E(t)$

$$E^\epsilon = E + \sigma \times \text{random}(1), \tag{5.1}$$

where σ is the standard deviation given by $\sigma = \frac{p}{100} \times \max_{t\in[0,T]} |B(t)|$, $p\%$ denotes the percentage of noise, and random(1) generates random values from a normal distribution with zero mean and unit standard deviation.

We consider examples with the terminal time $T = 1$, $x_0 = 0.2$, and the mesh size $h = \tau = 0.01$. The tolerance $\gamma = h^3 = 10^{-6}$ is used to stop the iteration of the predictor-corrector method in (4.12).

5.1 Example 1

We take the input data as

$$f(x,t) = 0, \quad \varphi(x) = \cos(\pi x), \quad E(t) = e^{-t}\cos\left(\frac{\pi}{5}\right).$$

One can easily check that the conditions of Theorems 3.1 and 3.2 are satisfied and hence the existence of a unique solution guaranteed. In fact, the analytical solution to the inverse problem (2.3) and (2.4) is given by

$$B(t) = \frac{1}{\pi^4}, \quad u(x,t) = e^{-t}\cos(\pi x). \tag{5.2}$$

For noiseless data $p = 0$, Figures 1 and 2 illustrate the convergence of the numerical solutions for $B(t)$ and $u(x,t)$ toward the corresponding analytical solutions (5.2), as the mesh size $h = \tau$ decreases from 0.1 to 0.05 and to 0.01. The corresponding l^2-accuracy errors between the numerical and analytical solutions for the thermal grooving coefficient

$$\|B^{\text{numerical}} - B^{\text{analytical}}\|_{l^2} = \sqrt{\frac{1}{K}\sum_{k=1}^{K}[(B^k)^{\text{numerical}} - (B^k)^{\text{analytical}}]^2}, \tag{5.3}$$

and the l^∞ for the profile $u(x,t)$ have been obtained as $\{3.6\times10^{-4}, 1.8\times10^{-4}, 4.2\times10^{-5}\}$ and $\{9.9\times10^{-3}, 5.8\times10^{-3}, 1.3\times10^{-3}\}$ for $h = \tau\{0.1, 0.05, 0.01\}$, respectively. To test stability the data (5.1) is further perturbed by $p\% = 2\%$ random noise. The numerically obtained results for $h = \tau = 0.01$ are presented in Figure 3. For $p = 2$, the l^2-accuracy error for $B(t)$ has been obtained as 8.4×10^{-4}. Overall, the numerical results presented in Figures 1-3 indicate that the numerically obtained solution are stable and accurate.

5.2 Example 2

We take the input data as

$$f(x,t) = (\pi^2 + e^t)\cos(\pi x), \quad \varphi(x) = \cos(\pi x), \quad E(t) = e^t\cos\left(\frac{\pi}{5}\right).$$

One can easily check that the conditions of Theorem 3.2 are satisfied and hence the uniqueness of solution is guaranteed. In fact, the analytical solution to the inverse problem (2.3) and (2.4) is given by

$$B(t) = \frac{e^{-t}}{\pi^2}, \quad u(x,t) = e^t\cos(\pi x). \tag{5.4}$$

Figure 4 illustrates the comparison between the analytical solution (5.4) and the numerical results computed by the predictor-corrector method with the cubic spline approximation and the formula (4.13), for $p\% = 1\%$ noise. From this figure it can be seen that the predictor-corrector method regularized by the cubic spline approximation achieves stable and accurate results, while unstable oscillations are obtained using the finite-difference formula (4.13) with $\tau = 0.01$.

The numerical solutions to the thermal grooving coefficient $B(t)$ for $p = 0$ and $p = 2$ noise are presented in Figure 5 in comparison with the analytical solution (5.4). For more clarity, we have calculated the l^2-accuracy errors (5.3) between the numerical and analytical solutions for the thermal grooving coefficient and obtained the small values $\{0.87, 2.0\}\times10^{-3}$ for $p\% \in \{0, 2\}\%$ noise, respectively. These small errors and the illustration depicted in Figure 5 indicate that the numerically obtained solutions are stable and accurate.

5.3 Example 3

A more severe test of recovering a discontinuous thermal grooving coefficient is investigated in this example. We take the input data as

$$f(x,t) = 2t\cos(\pi x) + (1+t^2)\pi^2\cos(\pi x) \times \begin{cases} 2, & t \in \left[\frac{1}{4}, \frac{3}{4}\right] \\ 1, & \text{otherwise} \end{cases},$$

$$\varphi(x) = \cos(\pi x), \quad E(t) = (1+t^2)\cos\left(\frac{\pi}{5}\right).$$

One can easily check that the conditions of Theorem 3.2 are satisfied and hence the uniqueness of solution is guranteed. In fact, the analytical solution to the inverse problem (2.3) and (2.4) is given by

$$B(t) = \frac{1}{\pi^2} \times \begin{cases} 2, & t \in \left[\frac{1}{4}, \frac{3}{4}\right] \\ 1, & \text{otherwise} \end{cases}, \quad u(x,t) = (1+t^2)\cos(\pi x). \tag{5.5}$$

Figure 6 illustrates the good agreement between the analytical and numerical results for both noiseless data $p = 0$ and noisy data $p\% = 2\%$. The l^2-accuracy errors (5.3) are obtained as $\{1.1, 4.6\} \times 10^{-3}$ for $p\% \in \{0, 2\}\%$, respectively. These small errors and the illustration depicted in Figure 6 indicate that the numerically obtained solutions are stable and reasonably accurate.

6 Conclusion

Thermal grooving by transient surface diffusion has been considered. In this case, the surface diffusivity depends on time and is unknown. We have shown that within this model the time-dependent thermal grooving coefficient $B(t)$ defined by (2.5) can be uniquely identified from the time-history recording of the profile at a single spatial location. The inverse problem is also known to be well-posed for smooth ideal input profile data. However, since in practice the measured data is always contaminated with noise then some sort of regularization needs to be performed to filter the noise and make the process of numerical differentiation well-posed. This has been achieved by a cubic spline technique. Numerical results presented and discussed for a couple of test examples involving smooth and discontinuous coefficients show that accurate and stable solutions have been achieved. Future work will consider a zero-curvature boundary condition $u_{xx} = 0$, [3], instead of $u_{xxx} = 0$ at the root $x = 0$, for which the resulting spectral problem is no more self-adjoint for any boundary condition at $x = 1$. In this case, the Fourier method in terms of eigenvalues and associated eigenfunctions needs further investigation.

Acknowledgements

The authors would like to acknowledge the support of the Fundamental Research Funds for the Central Universities (No. 3207012008A3) for this work.

References

[1] M. Abu Hamed and A. Nepomnyashchy. Groove growth by surface diffusion. *Physica D*, 298-299:42–47, 2015.

[2] O. Akyildiz and T. Ogurtani. Thermal grooving by surface diffusion: a review of classical thermo-kinetics approach. *Hittite Journal of Science and Engineering*, 4(1):7–16, 2017.

[3] D. Amram, L. Klinger, N. Gazit, H. Gluska, and E. Rabkin. Grain boundary grooving in thin films revisited: The role of interface diffusion. *Acta Materialia*, 69:386–396, 2014.

[4] T. Aziz, K. Arshad, and R. Jalil. Spline methods for the solution of fourth-order parabolic partial differential equations. *Applied Mathematics and Computation*, 167(1):153–166, 2005.

[5] B. Bialecki and G. Fairweather. Orthogonal spline collocation methods for partial differential equations. *Journal of Computational and Applied Mathematics*, 128:55–82, 2001.

[6] B. Bialecki, G. Fairweather, A. Karageorghis, and J. Maack. A quadratic spline collocation method for the Dirichlet biharmonic problem. *Numerical Algorithms*, 83:165–199, 2020.

[7] P. Broadbridge and P. Tritscher. An integrable fourth-order nonlinear evolution equation applied to thermal grooving of metal surfaces. *IMA Journal of Applied Mathematics*, 53:249–265, 1994.

[8] H. Brunner. *Volterra Integral Equations: An Introduction to Theory and Applications*. Cambridge University Press, 2017.

[9] J. W. Cahn and J. E. Hilliard. Free energy of a nonuniform system I interfacial free energy. *The Journal of Chemical Physics*, 28(2):258–267, 1958.

[10] C. P. Calderón and T. A. Kwembe. Dispersal models. *Revista De La Unión Matemática Argentina*, 37(3):212–229, 1991.

[11] J. R. Cannon, Y. Lin, and S. Wang. Determination of source parameter in parabolic equations. *Meccanica*, 27(2):85–94, 1992.

[12] E. A. Coddington and N. Levinson. *Theory of Ordinary Differential Equations*. McGraw-Hill, New York, 1955.

[13] Z. C. Deng and L. Yang. An inverse problem of identifying the coefficient of first-order in a degenerate parabolic equation. *Journal of Computational and Applied Mathematics*, 235(15):4404–4417, 2011.

[14] D. Fishelov. Semi-discrete time-dependent fourth-order problems on an interval: error estimate. In *Numerical Mathematics and Advanced Applications - ENUMATH 2013*, pages 133–142. (eds. S. Deparis, D. Kressner, F. Nobile and M. Picassor), Lecture Notes in Computational Science and Engineering, Vol.103, Springer, Cham, 2015.

[15] D. J. Gomain. *Free Vibrations Analysis of Beams and Shafts*. Wiley, New York, 1975.

[16] T. Hamieh, Z. Khatir, and A. Ibrahim. Analytical solutions to the problem of the grain groove profile. *Nanoscience Technology*, 5(2):(10 pages), 2018.

[17] T. Hamieh, Z. Khatir, and A. Ibrahim. New solution of the partial differential equation of the grain groove profile problem in the case of evaporation/condensation. *Scientific Reports*, 9(10143):(17 pages), 2019.

[18] J. Hristov. Fourth-order fractional diffusion model of thermal grooving: integral approach to approximate closed form solution of the Mullins model. *Mathematical Modelling of Natural Phenomena*, 13(6):1–14, 2018.

[19] V. L. Kamynin and T. I. Bukharova. Inverse problems of determination of the right-hand side term in the degenerate higher-order parabolic equation on a plane. In *International Conference on Numerical Analysis and Its Applications*, pages 391–397, 2016.

[20] V. L. Kamynin and T. I. Bukharova. On inverse problem of determination the right-hand side term in higher order degenerate parabolic equation with integral observation in time. *IOP Conference series: Journal of Physics: Conference Series*, 937:012018, 2017.

[21] F. Kanca and M. I. Ismailov. The inverse problem of finding the time-dependent diffusion coefficient of the heat equation from integral overdetermination data. *Inverse Problems in Science and Engineering*, 20(4):463–476, 2012.

[22] B. B. King, O. Stein, and M. Winkler. A fourth-order parabolic equation modeling epitaxial thin film growth. *Journal of Mathematical Analysis and Applications*, 28(2):459–490, 2003.

[23] G. T. Kossioris and G. E. Zouraris. Fully-discrete finite element approximations for a fourth-order linear stochastic parabolic equation with additive space-time white noise. *Esaim Mathematical Modelling and Numerical Analysis*, 44(2):289–322, 2010.

[24] Y. Kuramoto and T. Tsuzuki. On the formation of dissipative structures in reaction–diffusion systems. *Progress of Theoretical Physics*, 54(3):687–699, 1975.

[25] L. A. Kurtz, D. G. Weinman, and A. K. Cline. The solution of a fourth-order partial differential equatio using the method of lines. *Applicable Analysis*, 5:201–206, 1976.

[26] T. A. Kwembe. Existence and uniqueness of global solutions for the parabolic equation of the bi-harmonic type. *Nonlinear Analysis*, 47(2):1321–1332, 2001.

[27] P. Martin. Thermal grooving by surface diffusion: Mullins revisited and extended to multiple grooves. *Quarterly of Applied Mathematics*, 67(1):125–136, 2009.

[28] R. K. Mohanty, S. Mckee, and D. Kaur. A class of two-level implicit unconditionally stable methods for a fourth order parabolic equation. *Applied Mathematics and Computation*, 309:272–280, 2017.

[29] W. W. Mullins. Theory of thermal grooving. *Journal of Applied Physics*, 28(3):333–339, 1957.

[30] W. W. Mullins and P. G. Shewmon. The kinetics of grain boundary grooving in copper. *Acta Metallurgica*, 7(3):163–170, 1959.

[31] M. Nassirou. *Surface Diffusivity Measurements on 8 mol. % $Y_2O_3-ZrO_2$ Bicrystals via Grain Boundary Grooving Experiments*. PhD Thesis, Case Western Reserve University, Pro Quest Dissertations Publishing, 3158191, 2005.

[32] M. Ran, T. Luo, and L. Zhang. Unconditionally stable compact theta schemes for solving the linear and semi-linear fourth-order diffusion equations. *Applied Mathematics and Computation*, 342:118–129, 2019.

[33] A. N. Sandjo, S. Moutari, and Y. Gningue. Solutions of fourth-order parabolic equation modeling thin film growth. *Journal of Differential Equations*, 259(12):7060–7283, 2015.

[34] G. I. Sivashinsky. Nonlinear analysis of hydrodynamic instability in laminar flames—I. derivation of basic equations. *Acta Astronautica*, 4:1177–1206, 1977.

[35] Y. B. Wang, X. Z. Jia, and J. Cheng. A numerical differentiation method and its application to reconstruction of discontinuity. *Inverse Problems*, 18(6):1461–1476, 2002.

[36] W. Wei, M. Wang, E. Ambrosi, A. Bricalli, M. Laudato, Z. Sun, X. Chen, and D. Ielmini. Surface diffusion-limited lifetime of silver and copper nanofilaments in resistive switching devices. *Nature Communications*, 10(1):81–88, 2019.

[37] M. Winkler. Global solutions in higher dimensions to a fourth-order parabolic equation modeling epitaxial thin-film growth. *Journal of Mathematical Analysis and Applications*, 62(4):575–608, 2011.

[38] G. Xu and J. Zhou. Asymptotic behavior for a fourth-order parabolic equation involving the hessian. *Zeitschrift für Angewandte Mathematik und Physik ZAMP*, 69(6), 2018.

[39] Y. You and M. Kaveh. Fourth-order partial differential equations for noise removal. *IEEE Transactions on Image Processing*, 9(10):1723–1730, 2000.

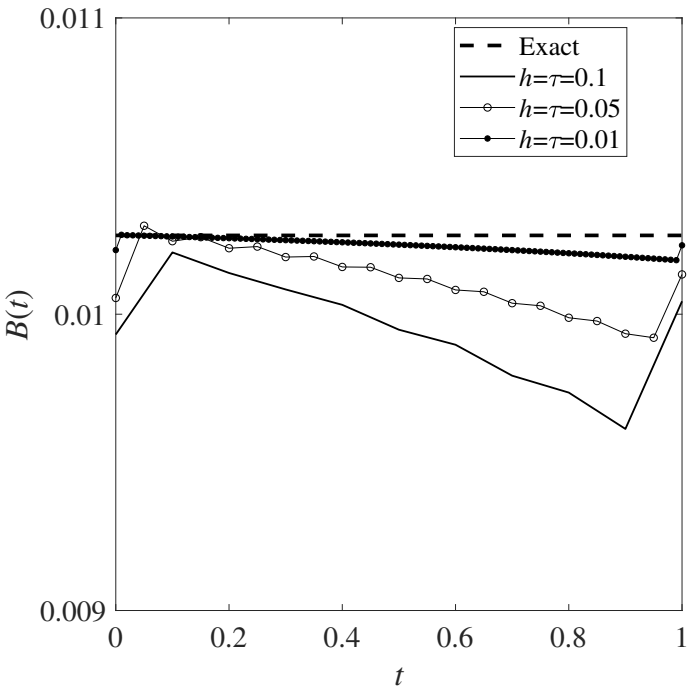

Figure 1: The exact and numerical solutions for the thermal grooving coefficient $B(t)$ for noiseless data $p = 0$ and various mesh sizes $h = \tau \in \{0.01, 0.05, 0.1\}$, for Example 1.

.

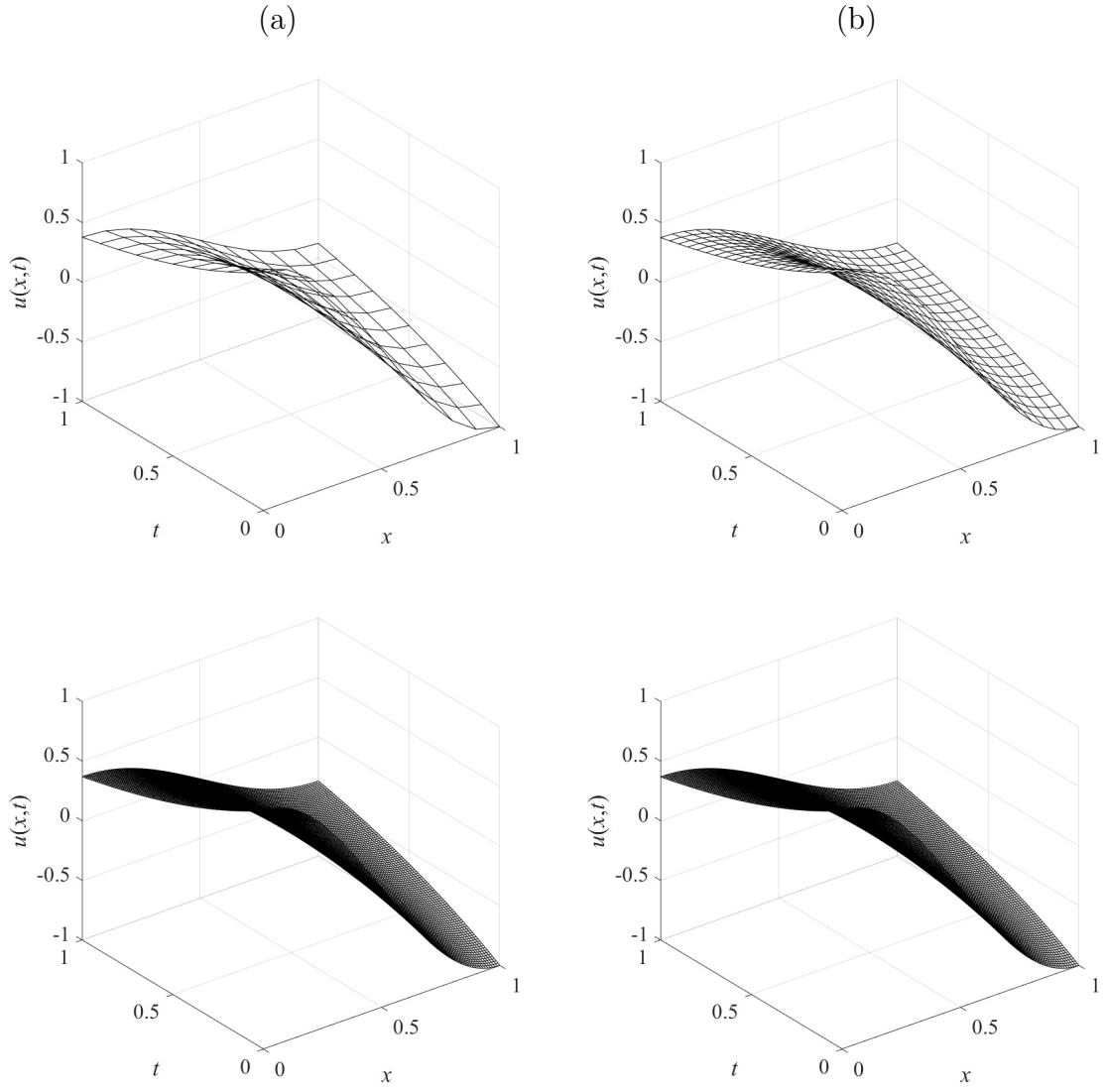

Figure 2: The exact and numerical solutions for the surface profile $u(x,t)$ for noiseless data $p = 0$ and various mesh sizes $h = \tau \in \{0.01, 0.05, 0.1\}$, for Example 1.

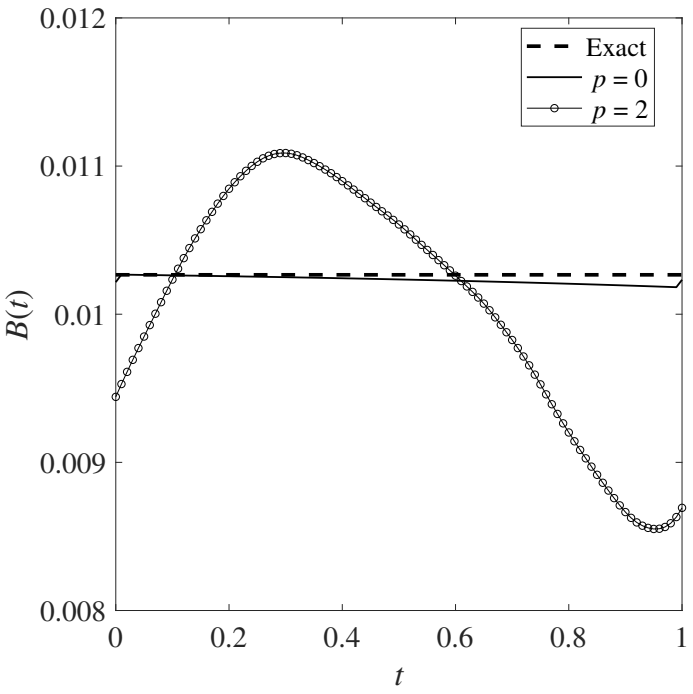

Figure 3: The exact and numerical solutions for the thermal grooving coefficient $B(t)$ for $p = 0$ and $p\% = 2\%$ noise and $h = \tau = 0.01$, for Example 1.

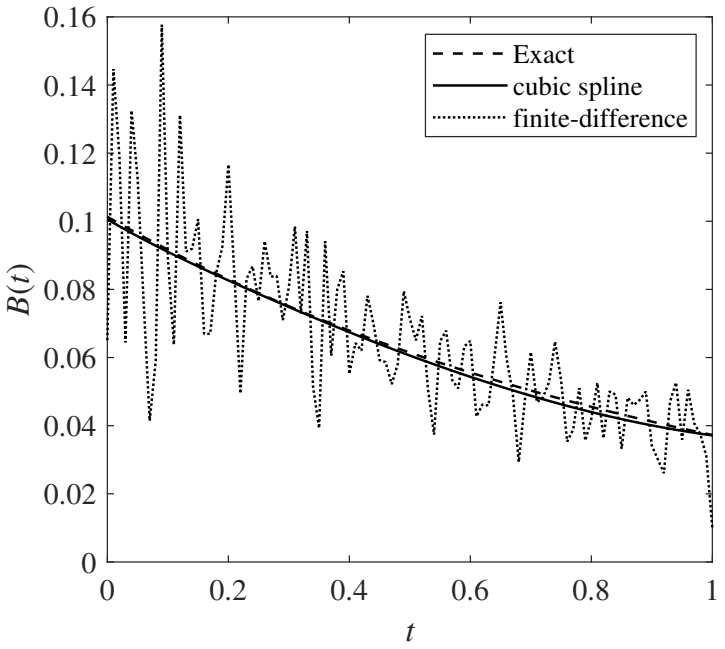

Figure 4: Comparison of the numerical solutions obtained by the predictor-corrector method with the cubic spline method (with $h = \tau = 0.01$) and the finite-difference formula (4.13), with $\tau = 0.01$, for $p\% = 1\%$ noise, for Example 2.

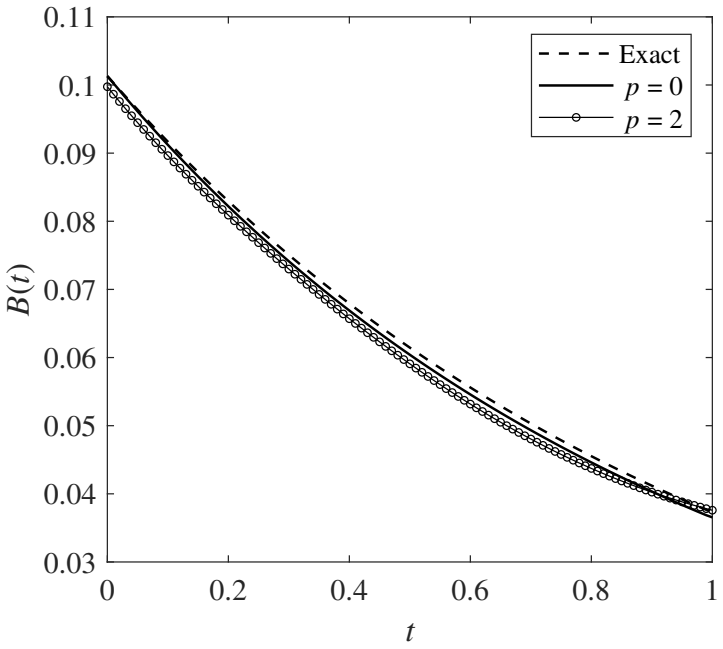

Figure 5: The exact and numerical solutions for the thermal grooving coefficient $B(t)$ for $p = 0$ and $p\% = 2\%$ noise and $h = \tau = 0.01$, for Example 2.

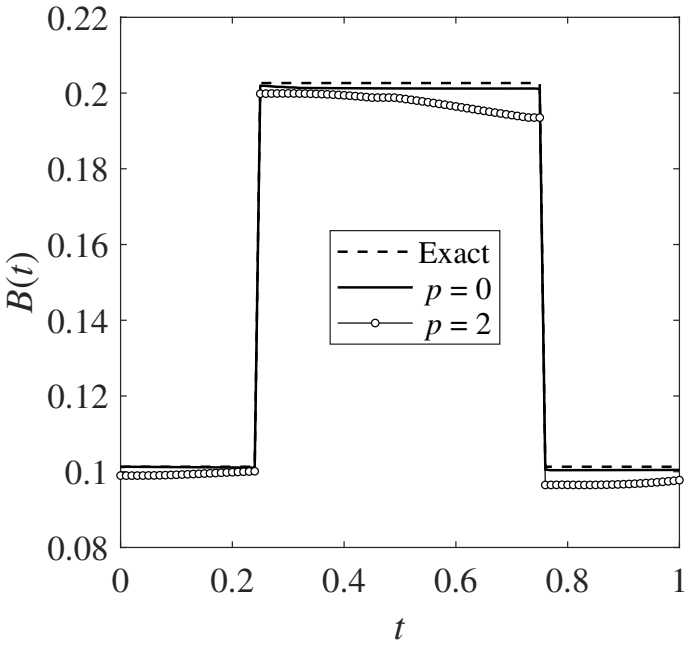

Figure 6: The exact and numerical solutions for the thermal grooving coefficient $B(t)$ for $p = 0$ and $p\% = 2\%$ noise and $h = \tau = 0.01$, for Example 3.